

Observation of five high-spin members of the $g_{9/2}f_{7/2}$ multiplet in ^{208}Pb

A. Heusler^{1,a}, G. Graw², Th. Faestermann³, R. Hertenberger², R. Krücken³, C. Scholl⁴, H.-F. Wirth³, and P. von Brentano⁴

¹ Max-Planck-Institut für Kernphysik, D-69029 Heidelberg, Germany

² Department für Physik, Ludwig-Maximilian-Universität München, D-85748 Garching, Germany

³ Physik Department E12, Technische Universität München, D-85748 Garching, Germany

⁴ Institut für Kernphysik, Universität zu Köln, D-50937 Köln, Germany

Received: 4 February 2010 / Revised: 12 March 2010

Published online: 14 April 2010 – © Società Italiana di Fisica / Springer-Verlag 2010

Communicated by J. Äystö

Abstract. In the doubly magic nucleus ^{208}Pb , five states are observed at 5648, 5658, 5686, 5694, 5836 keV by $^{208}\text{Pb}(p, p')$ via isobaric analog resonances in ^{209}Bi . The 5686, 5694, 5836 states with spins $6^-, 7^-, 8^-$ are shown to contain almost the full strength of the particle-hole configuration $g_{9/2}f_{7/2}$. The 5658 5^- state contains a major $g_{9/2}f_{7/2}$ fragment with admixtures of $d_{5/2}f_{5/2}$, $d_{5/2}f_{7/2}$. The 5648, 5649 keV states observed in a quintuplet at $E_x = 5.63 - 5.65$ MeV are preliminarily identified to have spins $(4)^-$ and 6^+ to 9^+ . The 5648 keV $(4)^-$ state contains almost half of the $g_{9/2}f_{7/2}$ strength and half of the $h_{9/2}d_{5/2}$ strength with admixtures of $d_{5/2}f_{5/2}$, $d_{5/2}p_{3/2}$, $d_{5/2}f_{7/2}$.

1 Introduction

Inelastic proton scattering on ^{208}Pb via isobaric analog resonances (IAR) in ^{209}Bi allows to determine the structure of particle-hole states in ^{208}Pb . The particle is chosen by adjusting the proton energy to an IAR; the amplitudes of the hole, coupling to the particle, are determined from the angular distribution of the outgoing protons in the reaction $^{208}\text{Pb}(p, p')$, see [1] and references therein.

High-resolution particle spectroscopy with the Q3D magnetic spectrograph at the München 14 MV tandem accelerator [2–4] allows to detect levels in $^{208}\text{Pb}(p, p')$ with low cross-section even in the vicinity of strongly excited levels [1].

Although the maximum cross-section of $^{208}\text{Pb}(p, p')$ via IAR in ^{209}Bi for states with dominant configuration $g_{9/2}f_{7/2}$ is lower by a factor of up to 100 than for many other states, five states of the multiplet predicted by the shell model at $E_x^{SM} = 5.77$ MeV are identified. Preliminary results are already included in the *Nuclear Data Sheets* [5].

The $g_{9/2}f_{7/2}$ multiplet expected at a high excitation energy is of special interest. The $f_{7/2}$ level is quite isolated from the other particle-hole levels with the same particle but other holes ($p_{1/2}$, $f_{5/2}$, $p_{3/2}$, $h_{9/2}$). Therefore on the $g_{9/2}$ IAR little mixing with other particle-hole configura-

tions built with the $g_{9/2}$ particle is expected. However, other neutron or proton configurations will admix.

2 Description of $^{208}\text{Pb}(p, p')$ via IAR

In the shell model, each particle-hole configuration is labeled $LJlj$ with particle $LJ = g_{9/2}, i_{11/2}, \dots$ and hole $lj = p_{1/2}, f_{5/2}, \dots$. The shell model energy $E_x^{SM}(LJlj)$ is derived from the single-particle states of the four neighboring nuclei [1]. Each state is identified by spin I , parity π and energy label E . The energy label is defined as the excitation energy rounded to units of keV. In order to have unique energy labels even for close doublets, sometimes 1 keV is added or subtracted.

The differential cross-section of $^{208}\text{Pb}(p, p')$ via an isolated IAR is described by a product of four factors [1,6]. One factor describes the population of the IAR with orbital momentum L and spin J as a function of the single-particle (s.p.) width $\Gamma_{LJ}^{s.p.}$, the total width Γ_{LJ}^{tot} and the resonance energy E_{LJ}^{res} (in the laboratory system). Another factor describes the decay of the IAR (the s.p. width $\Gamma_{lj}^{s.p.}$ and the phase between the interfering amplitudes of the decaying particles with orbital momentum l and spin j). A third factor describes the geometry of the angular momenta L, l and spins J, j recoupling to the final spin I . A fourth factor describes the Lorentzian shape of the resonance. Table 1 shows relevant parameters.

^a e-mail: A.Heusler@mpi-hd.mpg.de

Table 1. Parameters for IAR in ^{209}Bi . The uncertainty of Γ^{tot} (about 5–15 keV [7]) does not affect this work.

Isobaric analog resonance in ^{209}Bi						
Particle				Hole		
LJ	$E_{LJ}^{res(a)}$ MeV	$\Gamma_{LJ}^{tot(a)}$ keV	$\Gamma_{LJ}^{s.p.}$ keV	lj	$\Gamma_{lj}^{s.p.}$ keV	$E_{p'}^{SM}(LJlj)^{(f)}$ MeV
$g_{9/2}$	14.918	253	$20 \pm 1^{(a)}$	$p_{1/2}$	$28.6^{(a,c)}$	11.49
$i_{11/2}$	15.716	224	$2.2 \pm 0.3^{(b)}$	$f_{5/2}$	$5.2 \pm 0.4^{(b)}$	10.92
$j_{15/2}$	16.336	201	$0.7 \pm 0.3^{(b)}$	$p_{3/2}$	$14.6 \pm 0.5^{(b)}$	10.59
$d_{5/2}$	16.496	308	$45 \pm 5^{(a)}$	$i_{13/2}$	$0.06^{(d)}$	9.86
$s_{1/2}$	16.965	319	$45 \pm 8^{(a)}$	$f_{7/2}$	$0.67 \pm 0.04^{(e)}$	9.15
$g_{7/2}$	17.430	288	$45 \pm 10^{(a)}$	$h_{9/2}$	$0.04^{(d)}$	8.08
$d_{3/2}$	17.476	279	$35 \pm 10^{(a)}$			

(a) From [7].

(b) From [1].

(c) Reference value.

(d) Calculated [8].

(e) Equation (3).

(f) $E_{p'}^{SM}(LJlj) = E_{LJ}^{res} - E_x^{SM}(LJlj)$.

The measured angular distribution for $^{208}\text{Pb}(p, p')$ via IAR in ^{209}Bi can be fitted by a series of even-order Legendre polynomials P_K ,

$$\frac{d\sigma}{d\Omega}(E, I^\pi, \Theta, LJ) = \sum_K A_K(E, I^\pi, LJ) P_K(\Theta), \quad K = 0, 2, \dots \quad (1)$$

For states with pure particle-hole configurations such as $g_{9/2}f_{7/2}$ or $d_{5/2}f_{5/2}$, the anisotropy A_K/A_0 is entirely described by geometrical factors ($3j$ and $6j$ symbols) and the mean cross-section A_0 is proportional to $2I + 1$. In case several configurations contribute, the interference among them may change the angular distribution considerably.

For a state with energy label E , spin I and parity π , the angle-integrated cross-section of $^{208}\text{Pb}(p, p')$ taken on top of the IAR with angular momentum L and spin J is defined as

$$\sigma^{avg}(E, I^\pi, LJ) = \frac{1}{N} \sum_{i=1}^N \frac{d\sigma}{d\Omega}(E, I^\pi, \Theta_i, LJ). \quad (2)$$

It differs from the mean cross-section A_0 (eq. (1)). Namely the shape of the angular distribution is often pronounced (fig. 5) and the measured N data points do not cover the full range of scattering angles sufficiently well.

3 Experiments

By using the Q3D magnetic spectrograph at München, angular distributions and excitation functions for $^{208}\text{Pb}(p, p')$ were taken near all IAR in ^{209}Bi . In addition, spectra for $^{207}\text{Pb}(d, p)$ were taken at scattering angles $\Theta = 20^\circ, 25^\circ, 30^\circ$. Technical details are described in [1]. Excitation energies are determined with a precision

Table 2. For some members of the $g_{9/2}f_{7/2}$ multiplet and neighbouring states, energy label, spin, parity, excitation energy and mean cross-section of $^{208}\text{Pb}(p, p')$ (eq. (2)) on all IAR LJ in ^{209}Bi is given. By $^{208}\text{Pb}(n, n'\gamma)$ the excitation energies of the 5648, 5658 and 5694 members of the $g_{9/2}f_{7/2}$ multiplet are determined with higher precision while the 5836 state is not observed [5].

E	$I^\pi^{(*)}$	E_x [keV]	$\sigma^{avg}(E, I^\pi, LJ)$ [$\mu\text{b}/\text{sr}$]				
			$g_{9/2}$	$i_{11/2}$	$j_{15/2}$	$s_{1/2}$	$g_{7/2}$
5648	$(4)^-$	$5648.9 \pm 0.3^{(a)}$	5	20	15	4	4
5649	$6-9^+$	5649.3 ± 0.3		$^{(b)}$, see text			
5658	5^-	$5658.5 \pm 0.5^{(c)}$	10	8	15	13	16
5686	6^-	5686.1 ± 0.4	15	3	2	2	< 2
5690	4^+	$5690.0 \pm 0.6^{(d)}$	9	10	11	15	18
5694	7^-	$5694.4 \pm 0.4^{(e)}$	15	2	2	5	5
5836	8^-	5836.2 ± 0.4	12	2	5	6	5
5844	1^+	$5844.5 \pm 0.3^{(f)}$	4	6	5	3	3

(*) See text.

(a) 5649.01 ± 0.06 keV [5].

(b) Incompletely resolved doublet at $E_x = 5649$ keV.

(c) 5658.51 ± 0.04 keV [5].

(d) 5690.117 ± 0.023 keV [5].

(e) 5694.22 ± 0.12 keV [5].

(f) 5844.49 ± 0.20 keV [5].

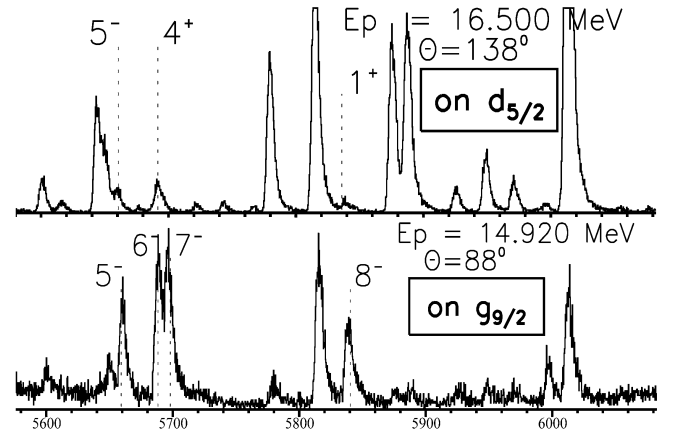


Fig. 1. Spectra of $^{208}\text{Pb}(p, p')$ taken at proton energies $E_p = 14.920$ MeV (on $g_{9/2}$ IAR) and $E_p = 16.500$ MeV (on $d_{5/2}$ IAR) for $5.60 < E_x < 6.10$ MeV. The 5658 5^- , 5686 6^- , 5694 7^- , 5836 8^- states are identified. In addition a 4^+ state [5] as member of the $E_x = 5.69$ MeV triplet and an 1^+ state [5] as member of the $E_x = 5.84$ MeV doublet are marked. The 5648 $(4)^-$ state as a member of the quintuplet at $E_x = 5.635-5.650$ MeV is not marked, see text. The structure of several other strongly excited states is being investigated, but not discussed in this paper.

of less than 1 keV by calibration with levels known from γ -spectroscopy [5] (table 2). The identification of the 5648 3^- or 4^- , 5649 6^+ to 9^+ , 5686 6^- , 5694 7^- , 5836 8^- states was already mentioned [5].

Figure 1 shows survey spectra in the range $5.6 < E_x < 6.1$ MeV taken on the $g_{9/2}$ and the $d_{5/2}$ IAR. Figures 2, 3 show spectra in the range $5.63 < E_x < 5.71$ MeV taken on

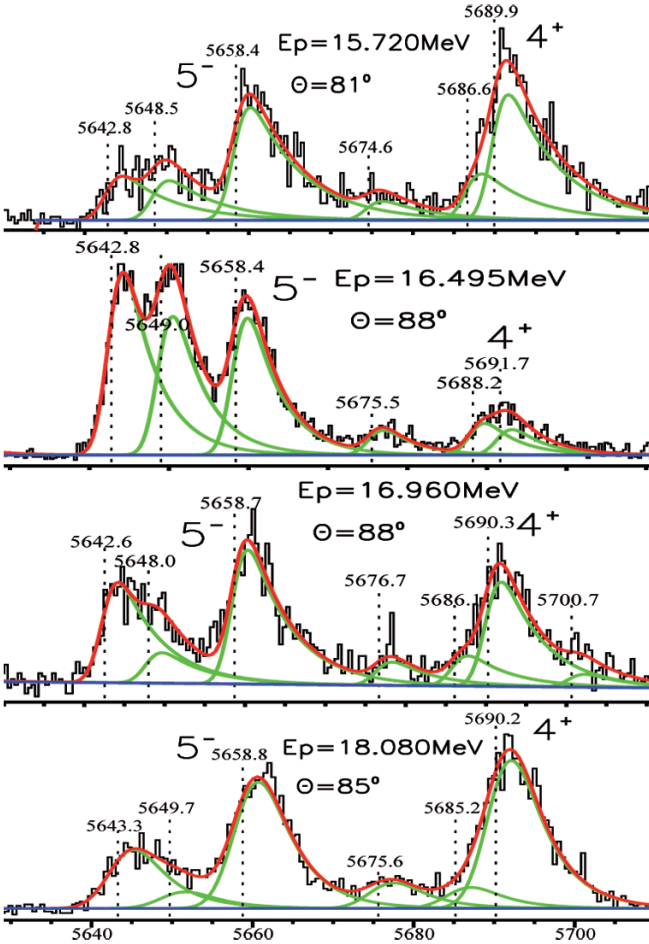


Fig. 2. (Color online) Spectra taken for $5.63 < E_x < 5.71$ MeV on the $i_{11/2}$, $d_{5/2}$, $s_{1/2}$, and beyond the $d_{3/2}$ IAR (from top to bottom). The 5658 5^- state and the 4^+ state [5] of the $E_x = 5.69$ MeV triplet are identified.

the $g_{9/2}$, $i_{11/2}$, $d_{5/2}$, $s_{1/2}$ IAR and far off resonance. They are fitted by GASPAN [9]; details of the computer code are described in [1]. The 5^- , 6^- , 7^- members of the $g_{9/2}f_{7/2}$ multiplet and a 4^+ state [5] are identified. Figure 4 shows spectra in the range $5.76 < E_x < 5.91$ MeV taken near the $g_{9/2}$, on the $d_{5/2}$ IAR and fitted by GASPAN. The 8^- member of the $g_{9/2}f_{7/2}$ multiplet and a 1^+ state [5] are identified.

In figs. 1–4 no scale for the ordinate is given, since the cross-sections vary by a factor up to 5 for different scattering angles and by a factor up to 100 for different proton energies.

Remarkably, early experiments at a resolution of 9 keV and scattering angles $\theta = 20^\circ, 40^\circ, 60^\circ, 90^\circ$ using the Enge split pole magnetic spectrograph at Los Alamos [10] yield data for the 5^- , 6^- , 7^- , 8^- members of the $g_{9/2}f_{7/2}$ multiplet in agreement with the recent data (fig. 5). Especially the steep raise of the angular distribution for the 5836 8^- state at $\theta = 20^\circ$ is observed.

Excitation functions were taken across all IAR with proton energies $14.8 < E_p < 18.1$ MeV at several scatter-

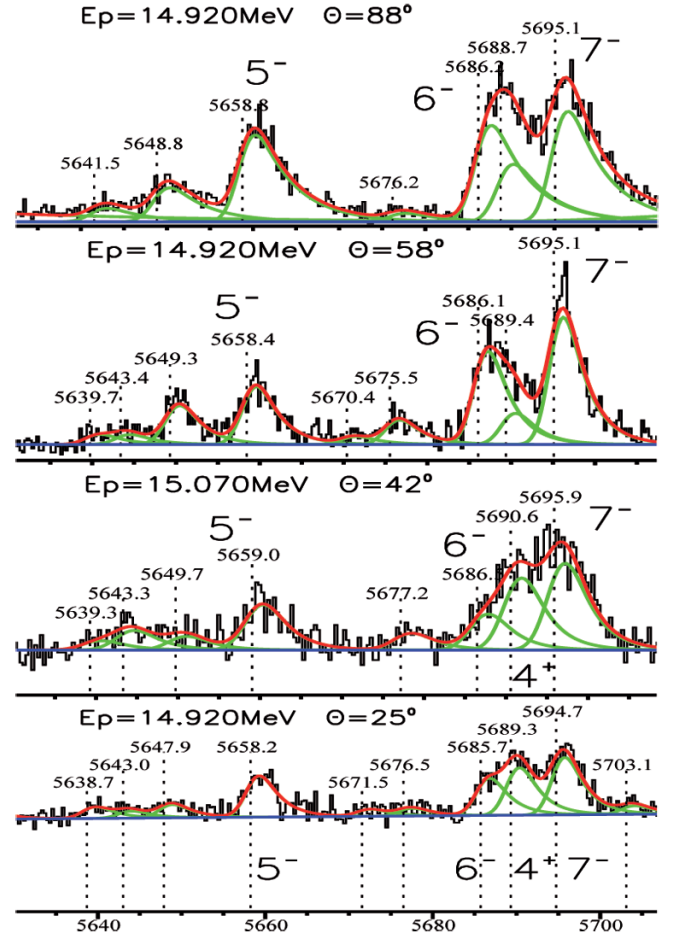


Fig. 3. (Color online) Spectra taken for $5.63 < E_x < 5.71$ MeV near the $g_{9/2}$ IAR at different scattering angles. The 5658 5^- state and the $E_x = 5.69$ MeV triplet with a 4^+ state [5] and the 6^- , 7^- states are identified. The 5648 (4^-) state as a member of the quintuplet at $E_x = 5.638$ – 5.650 MeV is not marked, see text. The background in the spectra taken at $\theta = 25^\circ, 42^\circ$ derives from $^1\text{H}(p, p)$.

ing angles. Mean cross-sections (eq. (2)) are given in table 2. Near the $g_{9/2}$ IAR spectra were taken at $E_p = 14.82$, 14.92 , 15.02 , 15.07 MeV covering the excitation function in the range of about 50–100% of the maximum cross-section at the chosen scattering angle.

Cross-sections were measured on all IAR in ^{209}Bi for scattering angles $20^\circ < \theta < 115^\circ$ and $\theta = 138^\circ$. The mean cross-section of $^{208}\text{Pb}(p, p')$ for some states varies by a factor up to 100, see, *e.g.*, the 5778 , 5874 , 5885 states in fig. 4. Since often a peak-to-valley ratio close to 1000 : 1 is obtained, cross-sections as low as $0.5 \mu\text{b}/\text{sr}$ can be measured even in distances less than 3 keV to strong levels at the low-energy side and in about 10 keV distance at the high-energy side. Contaminations from light nuclei (especially ^1H , ^2H , ^{12}C , ^{14}N , ^{16}O , ^{40}Ar) obscure some regions. Yet even here cross-section for stronger levels can be determined.

In the region $5.3 < E_x < 6.1$ MeV, by chance broad contamination lines from $^1\text{H}(p, p)$ with a width of $\delta E_x \approx$

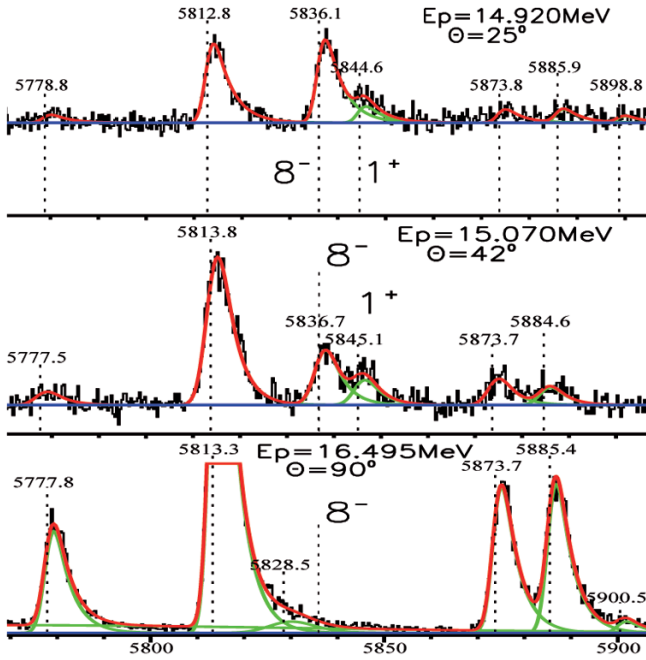


Fig. 4. (Color online) Spectra taken for $5.76 < E_x < 5.91$ MeV on $g_{9/2}$ IAR (top), near the $g_{9/2}$ IAR (middle), on $d_{5/2}$ IAR (bottom). The 1^+ state [5] and the 5836 8^- state of the $E_x = 5.84$ MeV doublet are identified. The background in the spectra taken near the $g_{9/2}$ IAR derives from ${}^1\text{H}(p, p)$.

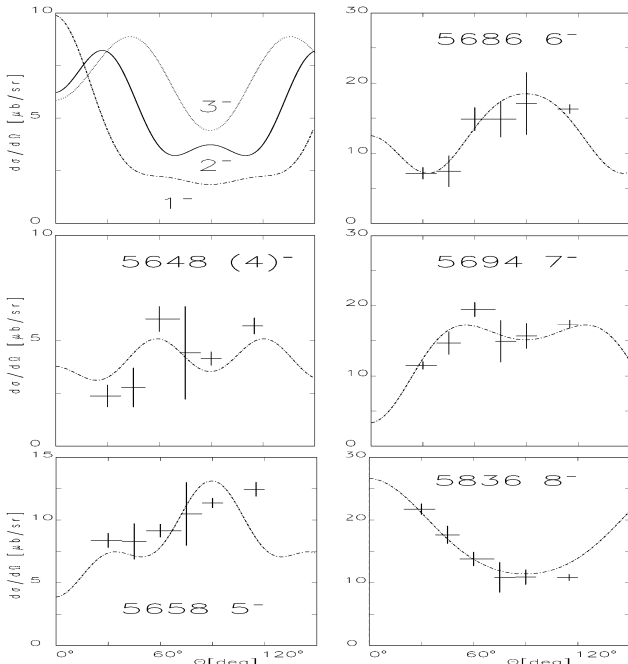


Fig. 5. Angular distribution for ${}^{208}\text{Pb}(p, p')$ on the $g_{9/2}$ IAR for the 5648, 5658, 5686, 5694, 5836 states. By using the IAR parameters from table 1, the drawn curves show calculated angular distributions assuming 40%, 70%, 90%, 90%, 100% $g_{9/2}f_{7/2}$ strength, respectively. The remaining strength is attributed to $h_{9/2}d_{5/2}$, $d_{5/2}f_{5/2}$, $d_{5/2}f_{7/2}$, $d_{5/2}h_{9/2}$, see text. Upper left panel: angular distributions for pure $g_{9/2}f_{7/2}$ configurations with spin 1^- , 2^- , 3^- at the predicted shell model energy ($E_x = 5.77$ MeV).

1.5 MeV obscure the spectra taken near the $g_{9/2}$ IAR for scattering angles $\Theta \approx 25^\circ$ – 50° . Hence in some spectra shown in figs. 3, 4 there is a large background.

Figure 5 shows angular distributions for the 5648 (4^-), 5658 5^- , 5686 6^- , 5694 7^- , 5836 8^- states. For convenience the calculated angular distributions for pure 1^- , 2^- , 3^- members of the $g_{9/2}f_{7/2}$ multiplet are shown, too.

4 Discussion

The 5686, 5694, 5836 states are selectively excited by the $g_{9/2}$ IAR. Near all other IAR the mean cross-section is less than on the $g_{9/2}$ IAR (table 2). Two of them are excited by ${}^{209}\text{Bi}(t, \alpha \gamma)$ [11], but none by ${}^{207}\text{Pb}(d, p \gamma)$ [11] or ${}^{207}\text{Pb}(d, p)$.

The 5.69 MeV triplet

Three states are seen in the region $5.68 < E_x < 5.70$ MeV (figs. 1, 2, 3). The 5690 state has spin 4^+ [5]. It is excited about equally strong at all proton energies E_p . The mean cross-section increases with E_p (table 2).

On the $g_{9/2}$ IAR, at almost all scattering angles, the 5686 and 5694 states are excited stronger than the 5690 4^+ state (figs. 2, 3). At $\Theta \approx 90^\circ$ the cross-section for both states is similar. However, the shapes of the angular distribution differ much for $30^\circ < \Theta < 60^\circ$ (fig. 5).

The 5694 state

The shape of the angular distribution for the 5694 7^- state can be well fitted by a pure $g_{9/2}f_{7/2}$ configuration (fig. 5). The anisotropy coefficients are $A_2/A_0 = -0.317$, $A_4/A_0 = -0.420$, $A_6/A_0 = -0.041$. The mean cross-section A_0 is given by eq. (1). The state is excited by the $g_{9/2}$ IAR only, hence no other neutron particle-hole configuration is present. In the ${}^{209}\text{Bi}(t, \alpha \gamma)$ experiment [11] about 10% $h_{9/2}d_{5/2}$ strength is determined for the 5694 state [11]. By assuming 90% $g_{9/2}f_{7/2}$ strength and using the other IAR parameters from table 1, the value of the single-particle width with $lj = f_{7/2}$ is derived from the mean cross-section A_0 as

$$\Gamma_{f_{7/2}}^{s.p.} = 0.67 \pm 0.04 \text{ keV at } E_{p'}^{SM} = 9.15 \text{ MeV.} \quad (3)$$

The calculated change of the penetrability [8] because of the difference between the shell model energy $E_{p'}^{SM}$ and $E_{p'} = E_p - E_x(5694)$ is included.

The good agreement of the s.p. width $\Gamma_{f_{7/2}}^{s.p.}$ determined from experiment with calculations [8] gives confidence in the calculations of the penetrability. Namely for $lj = f_{5/2}, f_{7/2}$ the distance between the shell model energies $E_{p'}^{SM}(lj)$ amounts to 1.8 MeV (table 1) and the penetrability depends essentially only on the orbital angular momentum l .

The 5686 state

By using the single-particle width $\Gamma_{f_{7/2}}^{s.p.}$ (eq. (3)), the angular distribution for the 5686 6^- state can be well fitted by $g_{9/2}f_{7/2}$ with 90% strength besides 10% $h_{9/2}d_{5/2}$ strength [11] (fig. 5).

The 5836 state

Two states are seen in the region $5.83 < E_x < 5.85$ MeV (figs. 1, 4), $E = 5836, 5844$.

The known 5844 1^+ state [5] is excited equally at all proton energies E_p ; the mean cross-section is rather small (table 2). At half maximum of the $g_{9/2}$ IAR ($E_p = 15.07$ MeV) and $\Theta = 42^\circ$ the cross-section of the 8^- state and the 1^+ state are similar, but on the $g_{9/2}$ IAR the 5836 state is much stronger excited (fig. 4). The angular distribution for the 5836 8^- state can be well fitted by a pure $g_{9/2}f_{7/2}$ configuration (fig. 5).

The 5658 state

In the region $5.65 < E_x < 5.67$ MeV (figs. 1, 2, 3) the 5658 5^- state is identified [5]. By assuming dominant configuration $g_{9/2}f_{7/2}$, the angular distribution is approximately fitted (fig. 5). Apparently the $g_{9/2}f_{7/2}$ strength is not complete and the shape is distorted by admixtures of $g_{9/2}p_{1/2}$, $g_{9/2}f_{5/2}$, $g_{9/2}p_{3/2}$.

About 0.5% $g_{9/2}p_{1/2}$ strength is determined in the $^{207}\text{Pb}(d,p)$ experiment. No excitation by $^{209}\text{Bi}(t,\alpha\gamma)$ or $^{207}\text{Pb}(d,p\gamma)$ is reported [11]. From the fit of the angular distribution taken on the $d_{5/2}$ IAR, an admixture of about 20% $d_{5/2}f_{5/2}$ is derived. Admixtures of $d_{5/2}f_{7/2}$, $d_{5/2}h_{9/2}$ are certainly present however, since the shape differs from a pure $d_{5/2}f_{5/2}$ configuration.

The 5.64 MeV quintuplet

In the region $5.63 < E_x < 5.65$ MeV (figs. 1, 2, 3) five states are observed with spins [5], i) 1^- , ii) 1 or 2^+ , iii) 2^- to 7^- , iv) 3^- or 4^- , v) 6^+ to 9^+ . We do not discuss the structure of these states in detail but mention that some of them are excited by the $g_{9/2}$, $j_{15/2}$, $d_{5/2}$ IAR quite differently, see figs. 2, 3.

While the 5648 state is excited by the $g_{9/2}$ and $d_{5/2}$ IAR, the 5649 state is excited by the $j_{15/2}$ IAR and contains a major $j_{15/2}p_{3/2}$ fraction, hence the parity is determined. By assuming spin 4^- , the angular distribution for the 5648 state taken on the $g_{9/2}$ IAR is fitted by 40% $g_{9/2}f_{7/2}$ strength (fig. 5).

The angular distribution for the 5648 $(4)^-$ state and for the 5649 state taken near the $j_{15/2}$, $d_{5/2}$ IAR add incoherently because the parity differs. The two angular distributions are difficult to disentangle, but upper limits of 20% $d_{5/2}f_{5/2}$, 20% $d_{5/2}f_{7/2}$ strength, 10% $d_{5/2}p_{3/2}$ strength in the 5648 state are derived.

Upper limits of 0.5% $g_{9/2}p_{1/2}$ or $g_{7/2}p_{1/2}$ strength are derived from a weak $^{207}\text{Pb}(d,p)$ excitation for the 5648 state. By assuming spin 4^- , from $^{209}\text{Bi}(t,\alpha\gamma)$ about 50% $h_{9/2}d_{5/2}$ strength is derived [11]. Hence the full configuration strength for the 5648 state is explained by about equal contributions of $g_{9/2}f_{7/2}$ and $h_{9/2}d_{5/2}$ with minor $d_{5/2}f_{5/2}$, $d_{5/2}p_{3/2}$, $d_{5/2}f_{7/2}$ components.

Identified $g_{9/2}f_{7/2}$ strengths and configuration admixtures

By using the IAR parameters from table 1 and the calculated change of the penetrability [8], the $g_{9/2}f_{7/2}$ strength in the 5658 5^- , 5686 6^- , 5694 7^- , 5836 8^- states is determined as 0.70 ± 0.10 , 0.90 ± 0.05 , 0.90 ± 0.05 , $0.95 < 1.00$, respectively. A preliminary evaluation assigns spin 4^- to the 5648 state with about 40% $g_{9/2}f_{7/2}$ strength.

From the angular distribution taken on the $d_{5/2}$ IAR, small admixtures of the configurations $d_{5/2}lj$, $lj = p_{3/2}$, $f_{5/2}$, $f_{7/2}$, $h_{9/2}$ for the 5648 $(4)^-$, 5658 5^- , 5686 6^- , 5694 7^- states are derived.

In the $^{207}\text{Pb}(d,p\gamma)$ experiment [11] none of the states with major $g_{9/2}f_{7/2}$ strength ($E = 5648, 5658, 5686, 5696, 5836$) is observed. In the $^{207}\text{Pb}(d,p)$ experiment weak $g_{9/2}p_{1/2}$, $g_{7/2}p_{1/2}$ components are derived for the 5648 $(4)^-$, 5658 5^- states.

In the $^{209}\text{Bi}(t,\alpha\gamma)$ experiment [11] about 50%, 10%, 10% $h_{9/2}d_{5/2}$ strength for the 5648 $(4)^-$, 5686 6^- , 5694 7^- states is derived, while the 5658 5^- , 5836 8^- states are not observed.

5 Summary

In the region $5.59 < E_x < 5.85$ MeV of the doubly magic nucleus ^{208}Pb , five states with major $g_{9/2}f_{7/2}$ fractions are identified. Three states are shown to contain almost the full $g_{9/2}f_{7/2}$ strength with spins 6^- , 7^- , 8^- . The known 5^- 5658 state is shown to contain about 70% of the $g_{9/2}f_{7/2}$ strength with admixtures of $g_{9/2}p_{1/2}$, $d_{5/2}f_{5/2}$, $d_{5/2}f_{7/2}$, $d_{5/2}h_{9/2}$. The 5648 state as member of a 15 keV quintuplet is identified as a $(4)^-$ state containing almost half of the $g_{9/2}f_{7/2}$ strength and half the strength of the proton configuration $h_{9/2}d_{5/2}$ together with some admixtures of $d_{5/2}f_{5/2}$, $d_{5/2}p_{3/2}$, $d_{5/2}f_{7/2}$.

The 1^- , 2^- , 3^- states with major $g_{9/2}f_{7/2}$ fractions are not yet located. Some of them are concealed in the quintuplet at $5.63 < E_x < 5.65$ MeV, others mix with the known states in the region at $E_x = 5.65\text{--}6.05$ MeV.

We thank T. von Egidy, J. Jolie, K.-H. Maier, D. M"ucher, N. Pietralla, F. Riess, V. Werner for discussions. This work has been supported by DFG Br799/20-1 and DFG Gr894/3.

References

1. A. Heusler, G. Graw, R. Hertenberg, F. Riess, H.-F. Wirth, T. Faestermann, R. Krücken, J. Jolie, D. Mücher, N. Pietralla, P. von Brentano, Phys. Rev. C **74**, 034303 (2006).
2. M. Löffler, H. J. Scheerer, H. Vonach, Nucl. Instrum. Methods B **111**, 1 (1973).
3. J. Ott, H. Angerer, T. von Egidy, R. Georgii, W. Schauer, Nucl. Instrum. Methods A **367**, 280 (1995).
4. H.-F. Wirth, PhD Thesis, Technische Universität München (2001) <http://tumb1.biblio.tu-muenchen.de/publ/diss/ph/2001/wirth.html>.
5. M.J. Martin, Nucl. Data Sheets **108**, 1583 (2007).
6. A. Heusler, H. L. Harney, J. P. Wurm, Nucl. Phys. A **135**, 591 (1969).
7. W.R. Wharton, P. von Brentano, W.K. Dawson, P. Richard, Phys. Rev. **176**, 1424 (1968).
8. R.G. Clarkson, P. von Brentano, H.L. Harney, Nucl. Phys. A **161**, 49 (1971).
9. F. Riess, <http://www.physik.uni-muenchen.de/~Riess/>.
10. P. Richard, P. von Brentano, H. Wieman, W. Wharton, W.G. Weitkamp, W.W. McDonald, D. Spalding, Phys. Rev. **183**, 1007 (1969).
11. M. Schramm, K.H. Maier, M. Rejmund, L.D. Wood, N. Roy, A. Kuhnert, A. Aprahamian, J. Becker, M. Brinkman, D.J. Decman, E.A. Henry, R. Hoff, D. Manatt, L. G. Mann, R.A. Meyer, W. Stoeffl, G.L. Struble, T.-F. Wang, Phys. Rev. C **56**, 1320 (1997).